Heliyon 10 (2024) e37481

Contents lists available at ScienceDirect

Heliyon

journal homepage: www.cell.com/heliyon

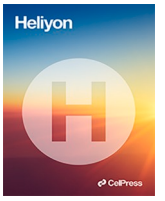

Research article

Metallic nanoentities: Bio-engineered silver, gold, and silver/gold bimetallic nanoparticles for biomedical applications

Sumbul Mujahid [a], Nida Ambreen [a,*], Muhammad Yaseen [a], Muhammad Ihtesham [b], Khalid Mohammed Khan [c], Muhammad Nasimullah Qureshi [d]

[a] Department of Chemistry, Abdul Wali Khan University Mardan, Mardan, 23200, Pakistan
[b] Department of Biotechnology, Abdul Wali Khan University Mardan, Mardan, 23200, Pakistan
[c] H. E. J. Research Institute of Chemistry, International Center for Chemical and Biological Sciences, University of Karachi, Karachi, 75270, Pakistan
[d] Department of Chemistry, University of Swabi, Swabi, 23561, Pakistan

ARTICLE INFO

Keywords:
Tamarix aphylla
Silver nanoparticles
Gold nanoparticles
Nanomedicine
α-amylase
Antioxidant
α-glucosidase
HRBCs hemolysis

ABSTRACT

This present study reports the biogenic synthesis of silver nanoparticles (AgNPs), gold nanoparticles (AuNPs) and Ag/Au bimetallic nanoparticles (BNPs) using bark extract of plant *Tamarix aphylla* (T.A). The bark extract contained total polyphenolic compounds and total flavonoids as 0.0362 mg/mg and 0.2928 mg/mg of the dried bark extract respectively. Silver nitrate ($AgNO_3$) and hydrogen tetra chloroaurate trihydrate ($HAuCl_4.3H_2O$) were used as precursors while deionised water and methanol (CH_3OH) were used as solvents. Synthesized nanoparticles were characterized through UV–visible spectroscopy, SEM (scanning electron microscopy), TEM (transmission electron microscopy) and FTIR (Fourier transform infrared) for their morphology, structure, and identification of different functional groups. The UV–visible spectra of AgNPs, AuNPs and Ag/Au BNPs showed peaks at 436, 532 and 527 nm respectively due to the excitation of Surface Plasmon Resonance. SEM and TEM images showed spherical and well distributed nanoparticles (NPs) with particle size as 29 nm (AgNPs), 13 nm (AuNPs) and 26 nm (Ag/Au BNPs). The synthesized NPs are significantly active against inhibition of free radicals, α-amylase, α-glucosidase and have anti inflammatory potential with AgNPs having the highest percent activity at 400 μg/ml, followed by Ag/Au BNPs. The same trend (AgNPs > Ag/AuBNPs > AuNPs) has been observed at all concentrations i.e. 100 μg/ml, 200 μg/ml and 400 μg/ml. AuNPs have shown lowest activity at all concentrations. So the current study strongly confirms use of T.A bark extract as reducing agent for synthesis of metal NPs and opens up a new possibility of using these green synthesized NPs as biomedicines. We also suggest further *in vivo* investigation to report any side effects if present.

1. Introduction

Nanoparticles (NPs), ranging in size from 1 to 100 nm in one of their dimensions, have been into use for a variety of pharmacological applications due to their abundant versatile properties accredited to their nano scale size [1]. NPs of different metals have

* Corresponding author.
E-mail addresses: sumbul_mujahid@yahoo.com (S. Mujahid), nidaambreen@awkum.edu.pk, nidahej@yahoo.com (N. Ambreen), yaseen.chemist@gmail.com (M. Yaseen), m.ihtesham222@gmail.com (M. Ihtesham), khalid.khan@iccs.edu (K. Mohammed Khan), mnasimuq@yahoo.com, mnasimuq@uoswabi.edu.pk (M. Nasimullah Qureshi).

https://doi.org/10.1016/j.heliyon.2024.e37481
Received 20 May 2024; Received in revised form 4 September 2024; Accepted 4 September 2024
Available online 7 September 2024

exhibited significant therapeutic advantages in the field of medicine [2], agriculture [3,4] etc. Silver nanoparticles (AgNPs) and gold nanoparticles (AuNPs) have gained tremendous attention by the researchers because of their unique properties such as size and high surface area [5]. Multipurpose applications of AgNPs have previously been reported such as the antitumor effect, antibiotics, antimicrobial effect, pollution treatment, molecular switches, electronics, materials science, forensic science, textile industry, food technology, agriculture, catalytic, drug delivery, anti-cancer, sensing diseases diagnosis, therapeutic applications, anti-microbial effect, anti mosquitoes, antibacterial etc [6–9]. Similarly, AuNPs have been considered efficient because they are less toxic, goes well with the hormony of the human body and has a high surface area that can be effortlessly adapted [10]. There are a number of chemical and physical methods to synthesize NPs but we have chosen the green method. Green or biogenic synthesis of NPs means that for the reduction of metals to bring them into nano scale; plants, fungi, algae, microorganisms etc are used and not hazardous chemicals because they are expensive, time consuming and generates harmful residues to the environment. Green synthesis of NPs employing extracts of plants is reflected as easy, inexpensive, and biodegradable method [11–13]. The compounds present in the plant extracts, mostly polyphenolic compounds, act as reducing and stabilizing agents. Published research work has shown that the capping agents which stops the synthesized nanoparticles from aggregation includes amino acids and polysaccharides [14]. Different plant extracts have been successfully employed in the preparation of silver and gold NPs [12,15–17] and they have given promising results in a number of biological activities such as antimicrobial [18], antioxidant, antibacterial [19], antileishmanial [20] etc. *Tamarix aphylla* (T. A) is the major recognized species of the genus Tamarix, which can grow up to 18 m and is a widespread plant of the Tamaricaceae family. It is a rich source of phenolic compounds [21] and other phytochemicals like Benzeneselenol, Gibberellic acid, and Triaziquone. The bark of T.A is reported to have various useful phenolics [22] and â-sitosterol [23]. Leaves of T.A contain propenoic acid and beta-D-mannofuranose [24]. Different parts of the plant (T.A) have successfully been used for the synthesis of metal NPs [25–27]. Bimetallic Ag/Au nanoparticles (BNPs) have marvelous applications such as in electronics, optical, catalytic, structural and biomedical, that have gotten application in cosmetics and beauty care products, anticancer, cell reinforcement, and antimicrobial drugs [28]. Nowadays, multimetallic nanoparticles are under study because of their electronic, optical, magnetic, and catalytic properties which are different from the individual components. In order to bring about amendments in the properties of AgNPs and AuNPs, the synthesis of Ag/Au BNPs came into being. Ag/Au BNPs show better catalytic and antimicrobial activities and surface-enhanced raman scattering (SERS) relative to the individual components, more sensing, greater increased resistive heating generation, improved tunable NIR absorption, and efficiency in photothermal ablation led to its applicability in *in vitro* and *in vivo* cancer therapy, among other things [29]. Several techniques are employed to create Ag/Au BNPs, including in situ co-reduction, sequential reduction, galvanic replacement reaction, core-shell nanoparticles, seed-mediated growth, electrochemical deposition, template-assisted synthesis, chemical linking or cross-linking, emulsion methods, hydrothermal or solvothermal synthesis, hybridization of pre-synthesized NPs [30]. Ag/Au BNPshave been synthesized by a number of scholars using green method and have confirmed their various potentials such as antileishmanial, anticancer, antibacterial, phytotoxicity, antimicrobial, cytotoxicity [31–36] (see Table 1).

By studying the literature and looking at the growing interest of plants derived NPs we in this paper have used the bark extract of T. A for the successful fabrication of Ag and Au NPs because this plant has several therapeutic advantages and bark part has been used for hepatitis and skin diseases [37]. In an *in-vivo* study the bark part has shown anti-inflammatory, anti-pyretic and anti-nociceptive activity [38] so we decided to use the bark part as a reducing and capping agent for metal NPs and then test the pharmacological efficacy of the synthesized NPs. To our knowledge this is the first attempt of using bark part to synthesize NPs. The fabricated NPs were characterized using techniques such as UV, SEM, TEM, FTIR for their morphology, structural elucidation and functional groups attached. Moreover, the prepared NPs were tested for biological activities such as antioxidant, α-amylase inhibition, α-glucosidase inhibition, HRBCs heat induced hemolysis. The content of total polyphenolic compounds and total flavonoids in the bark of T.A plant was also calculated which are actually responsible for the biogenic reduction of silver and gold in the synthesis of NPs.

2. Materials and methods

2.1. Chemicals and reagents

Chemicals such as silver nitrate ($AgNO_3$), gallic acid (>97 %), Folin-Ciocalteu reagent (2 N), methanol (CH_3OH), sodium carbonate (Na_2CO_3), Quercetin (98 %), potassium acetate (KCO_2CH_3), aluminium chloride ($AlCl_3$), distilled and deionised water, hydrogen tetra chloroaurate trihydrate ($HAuCl_4.3H_2O$) used in this research work were purchased from Sigma Aldrich (Steinheim Germany) and Merck (Darmstadt Germany) and were of analytical grade.

2.2. Collection of T.A Plant bark and preparation of extract

Bark of T.A was obtained from the Mayar region (latitude 34.167226, longitude 72.081465) of District and Tehsil Mardan, Khyber Pakhtunkhwa (KP) Pakistan and authenticated by Taxonomist Dr Mohib Shah, Associate Professor, Department of Botany, Abdul Wali Khan University Mardan (AWKUM). The bark was washed with distilled water to get rid of dust and debris. It was dried in shade and then ground to 2 mm mesh size. The plant extract (T.A bark) was prepared in deionised water under reflux with a plant to solvent ration of 1:10 for 2 h and then filtered. The dark brown extract obtained was stored in refrigerator.

Fig. 1. Colour change in the synthesis of AgNPs with the passage of time.

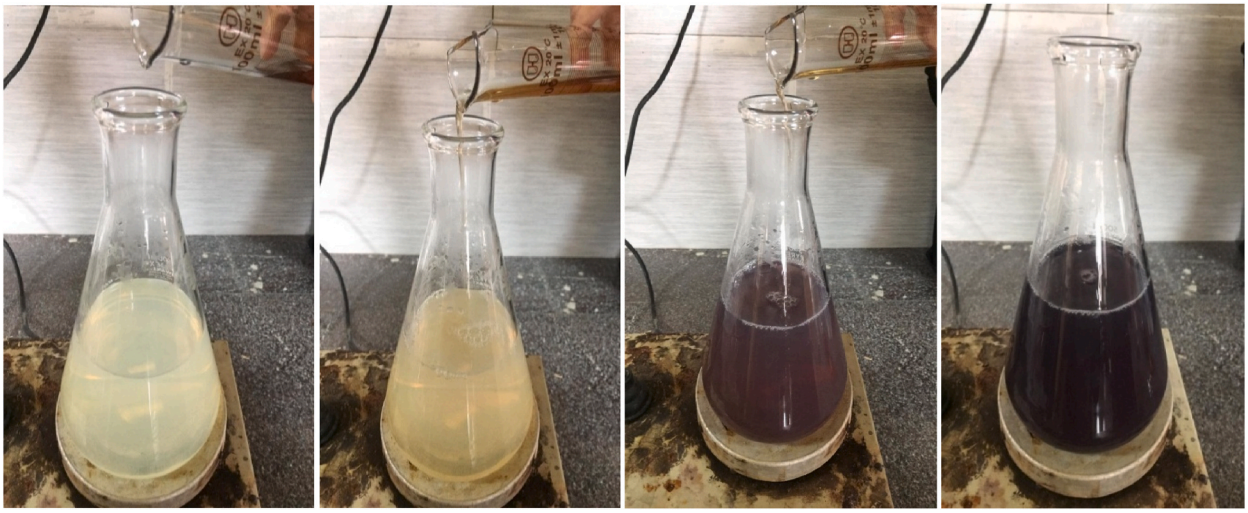

Fig. 2. Colour change in synthesis of AuNPs with the passage of time.

2.3. Determination of total polyphenolic compounds

Total polyphenols in bark of T.A plant were determined through Folin-Ciocalteau (FC) method [39]. A weighed amount of the dried extract was taken in 5 mL distilled water and then filtered. Solutions of standard gallic acid were also prepared in distilled water in range of 0.02–0.1 mg/mL 1 mL from each of the gallic acid solutions, plant extract solution and distilled water (DW) as blank was taken in separate test tubes and 5 mL FC reagent (prepared in DW in a ratio of 1:10) was added to test tubes. These were then allowed to react for 8 min and then 4 mL Na_2CO_3 (7.5 %) was added. Test tubes were stored in dark for 2 h and then solutions were measured at 740 nm using UV–Visible spectrophotometer to find the absorbance.

2.4. Determination of total flavonoid compounds

The quantity of all flavonoids were found following chang et al. [40]. Six different solutions of Quercetin as standard were prepared in the range of 0.02–0.08 mg/mL 10 mL methanol was taken and 1 gm extract was mixed with it and then filtered. 0.5 mL from each standard solution, plant extract solution and blank (methanol) was taken in separate test tubes. Then 0.1 mL potassium acetate (1 M), 2.8 ml distilled water, 1.5 mL methanol and 0.1 mL aluminium chloride (10 %) were introduced into theses test tubes. These solutions were then allowed to react for about 30 min in dark and then the absorbance was measured at 415 nm using UV–Visible spectrophotometer.

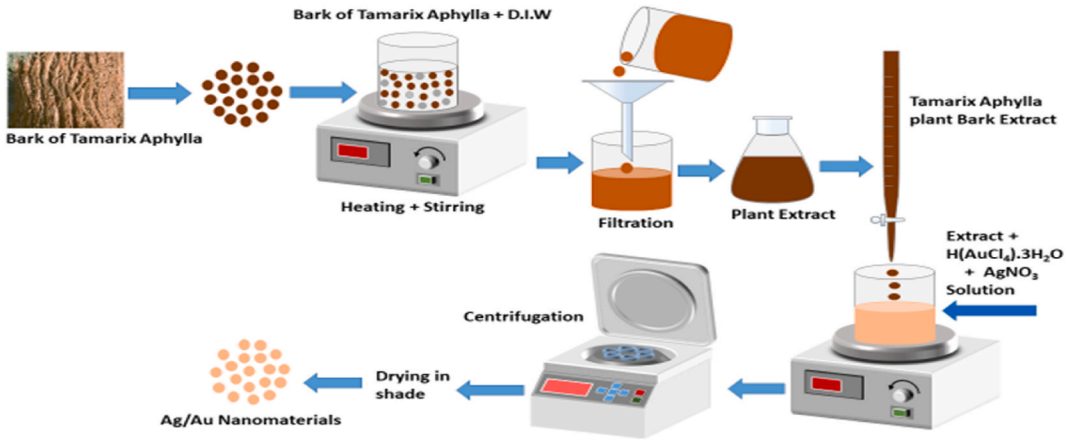

Scheme 1. Green synthesis of Ag/Au BNPs.

2.5. Green synthesis of AgNPs

The pathway for synthesis of AgNPs was green synthesis method. $AgNO_3$ solution and the plant extract were mixed in 1:10 ratio i.e. 1 mL of plant extract (T.A bark) was slowly introduced into 10 mL of 1 mM solution of silver nitrate solution in a conical flask. The solution was continuously stirred at 3 rpm and heated at 60 °C. The colour of the solution was observed which changed from light brown to reddish brown colour within 20 min, as shown in Fig. 1, clearly indicating the reduction of the Ag^{+} to Ag° and formation of AgNPs in the solution. The solution containing NPs was centrifuged at a speed of 14000 rpm for about 10 min. The particles were washed twice with deionised water and then separated and kept in dark for drying and to avoid the photoactivation. After drying the AgNPs were obtained and used for further analysis.

2.6. Green synthesis of AuNPs

Gold salt solution ($HAuCl_4.3H_2O$) and the plant extract (T.A plant bark) were blended in ration of 1:10 i.e. 1 mL of plant extract was added slowly into10 mL of 1 mM solution of gold solution ($HAuCl_4$) in a conical flask. The solution was continuously stirred at 3 rpm and heated at 60 °C. The colour of the solution as shown in Fig. 2 changed from light brown to purple within 10 min showing reduction of the Au^{+3} to Au° and formation of AuNPs in the solution. It was then centrifuged at 14000 rpm for about 10 min. AuNPs settled in the bottom and supernatant was discarded. The collected AuNPs were washed twice and then dried in shade.

2.7. Green synthesis of Ag/Au BNPs

In this method, silver nitrate solution ($AgNO_3$) and gold solution ($HAuCl_4.3H_2O$) were mixed with the extract (T.A plant bark) through a ratio of 4.5:4.5:1 i.e. 4.5 mL of each of silver nitrate solution ($AgNO_3$) and gold solution ($HAuCl_4.3H_2O$) were taken in 200 mL conical flask and 1 mL plant extract was added dropwise. The reaction was carried out with constant stirring at 3 rpm and at a temperature of 60 °C. The solution colour changed from light brown to purple, indicating the reduction of Au^{+3} to Au° and Ag^{+} to Ag°. The solution was then centrifuged at 14000 rpm for 10 min. The NPs pallet was washed twice with DW and dried in shade. Dried nanoparticles (Ag/Au BNPs) were then used for further analysis. The whole process for the preparation is represented schematically, in Scheme 1.

2.8. Characterization of the synthesized NPs

The synthesized NPs were examined and confirmed through UV, SEM, TEM and FTIR techniques. The UV analysis was done in such away by taking some quantity of the nanoparticles and dispersed it in ethanol solvent and then carried to UV–Visible Spectrophotometer Lambda-25 (PerkinElmer) for examination. External structure of prepared nanoparticles was confirmed via SEM model JSM-5910 JEOL. For the internal structure of the nanoparticles, TEM examination was carried out via transmission electron microscope (JEM 2100F, 200 kV). Similarly, FTIR analysis was examined through FTIR (Nicolet 1S5 USA, 400-4000 cm^{-1}).

2.9. Biological activities

The green synthesized NPs were further assessed in a series of biological assays such as antioxidant, antidiabetic (α-amylase inhibition and α-glucosidase inhibition) and anti-inflammatory (HRBCs heat induced hemolysis) in order to determine their biological potential.

Table 1
UV visible data of gallic acid and bark extract solutions.

Cocentration mg/ml	Absorbance
0.02	0.322
0.04	0.459
0.06	0.646
0.08	0.831
0.1	1.012
Bark extract 1	2.299
Bark extract 2	2.408
Bark extract 3	2.427
Average absorbance of bark extract	2.378

2.9.1. Antioxidant activity

Antioxidant assay was performed just like the method of Dybka-Stępień, K. et al. [41] with a little modification. For the preparation of stock solution we took 4 mg of DPPH reagent and dissolved it in 100 mL methanol (80 %). This solution was kept in dark at 4 °C. This experiment was used to assist the dose-dependent antioxidants activities of all the prepared NPs. For each NP, 100 μg/mL, 200 μg/mL, and 400 μg/mL solution was prepared and 50 μL was taken from each which was mixed with 100 μL of a 4 mM DPPH reagent against the standard Ascorbic acid in a 96-well plate. These solutions were kept at 25 °C for 30 min in a dark environment. After 30 min, absorbance of all the solutions was calculated at 517 nm using a UV–Vis ELISA plate reader.

$$\%\text{DPPH radical scavenging activity} = (A_0 - A_1) \ / \ A_0 \times 100$$

Here, A_0 represents absorbance of control and A_1 indicates absorbance of the sample.

2.9.2. Alpha amylase inhibition activity

Anti-diabetic potential of AgNPs, AuNPs and Ag/Au BNPs was determined through alpha amylase inhibitory assay as described by Ref. [42]. The samples (NPs) were screened at concentration i.e. 100 μg/mL, 200 μg/mL and 400 μg/mL. At first a fresh 0.5 % starch solution was prepared. From this starch solution, 100 μL was taken and added with 50 μL of alpha amylase (0.5 mg/mL) enzyme in the presence of test compounds. Acarbose was used as a reference drug while DMSO served as a blank. These solutions were incubated for 10 min at 37 °C. After 10 min, 100 μL of the DNS reagent (3,5-dinitrosalicylic acid) was added and reaction in solution continued for an additional for 5 min. After incubation, 90 °C heat was given for 15–20 min and then diluted with distilled water on an ice bath. Atlast ELISA plate reader measured the absorbance at 540 nm. The % α-amylase inhibition was determined by the following equation:

$$\%\ \alpha - \text{amylase inhibition} = (A_0 - A_1) \ / \ A_0 \times 100$$

Here, A_0 indicates absorbance of the control and A_1 indicates absorbance of the sample.

2.9.3. Alpha-glucosidase inhibition activity

Possible inhibition of α-glucosidase by AgNPs, AuNPs and Ag/Au BNPswere assessed through α-glucosidase inhibition assay according to optimized procedure of [42]. The substrate in this assay was *p*-nitro phenyl glucopyranoside (*p*NPG). We employed various solutions (100 μg/mL, 200 μg/mL, 400 μg/mL) of our NPs, mixing each one with 10 μL of alpha glucosidase (0.075 μg/mL) which were incubated at a temperature of 37 °C for 20 min. After 20 min, 125 μL phosphate buffer (0.2M, pH 6.8) was introduced to further incubate the mixture for an additional 20 min. After 20 min, 20 μL *p*NPG (3 mM) was introduced and we incubated the mixture again for 30 min at 37 °C. The reaction stopped when 50 μL sodium carbonate (0.1 N) was added and in the last UV–Vis ELISA plate reader measured the absorbance at 405 nm. Acarbose served as the standard control here. The calculations were done using the equation:

$$\%\ \alpha - \text{glucosidase inhibition} = (A_0 - A_1) \ / \ A_0 \times 100$$

Here, A_0 indicates absorbance of the control and A_1 indicates absorbance of the sample.

2.9.4. HRBCs heat induced hemolysis activity

The anti-inflammatory potential of all the prepared NPs was evaluated by human red blood cells (HRBCs). Briefly, 5 mL of fresh blood was diluted with PBS at 1:3 taken in EDTA tubes and obtained from a consented healthy donor. The blood was centrifuged at 3000 rpm for 10 min to separate RBCs. The RBCs collected were washed with PBS (pH 7.5) a couple of times until the supernatant became clear and discarded. Then RBCs suspension was made when diluted with PBS at 1:3. This RBCs suspension was treated with several concentrations of test samples i.e. 100 μg/mL, 200 μg/mL and 400 μg/mL. The mixture tubes when incubated at ambient temperature for 10 min were further incubated at 55 °C for 30 min. After the required time, the mixture samples were centrifuged at 3000 rpm for 10 min, and the free haemoglobin intensity was examined at 570 nm. In this assay PBS served as negative control, while Aspirin served as a reference drug. Using the following formula, the % hemolysis was determined:

$$\%\ \text{hemolysis inhibition} = (A_0 - A_1) \ / \ A_0 \times 100$$

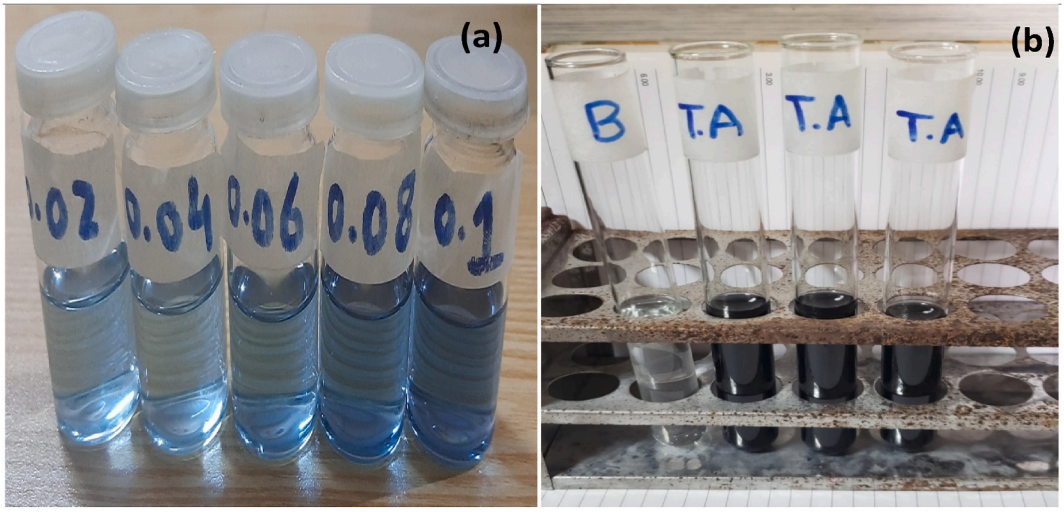

Fig. 3. Standard solutions of (a) gallic acid and (b) plant extract after 2 h.

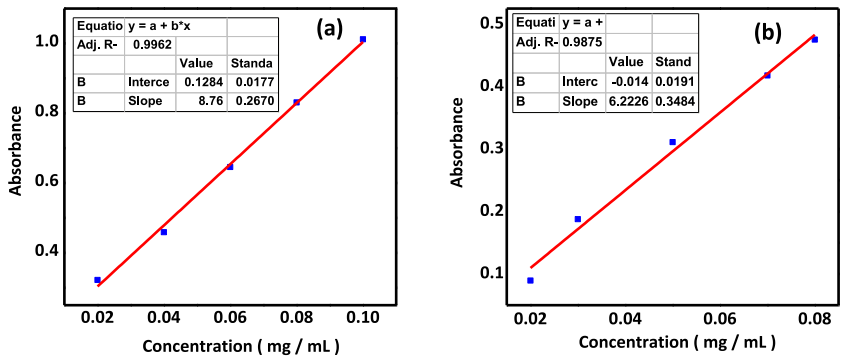

Fig. 4. (a) Total polyphenols and (b) Total flavonoids quantification standard calibration curve.

Table 2
UV visible data of Quercitin and bark extract solutions.

Cocentration mg/ml	Absorbance
0.02	0.0894
0.03	0.1877
0.05	0.3111
0.07	0.4178
0.08	0.4753
Bark extract 1	1.8433
Bark extract 2	1.7418
Bark extract 3	1.8390
Average absorbance of bark extract	1.8081

Here, A_0 is the absorbance of the control and A_1 is absorbance of the sample.

3. Results and discussion

3.1. Determination of total polyphenolic compounds

Folin-Ciocalteau assay was performed to measure total polyphenolic compounds Table 1. This assay was used because it quantifies the polyphenolic compounds very rapidly and interferes rarely in the solution. Gallic acid was used as a standard with 5 different concentrations as shown in Fig. 3a. Five points calibration curve was used to find the straight line equation where the concentrations of the standard solutions were plotted against their respective absorbance. The regression curve was obtained with R^2 as 0.99962 as

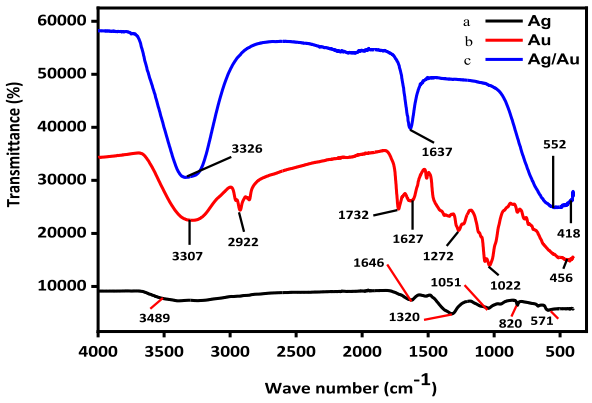

Fig. 5. FTIR results of (a) AgNPs, (b) AuNPs and (c) Ag/Au BNPs.

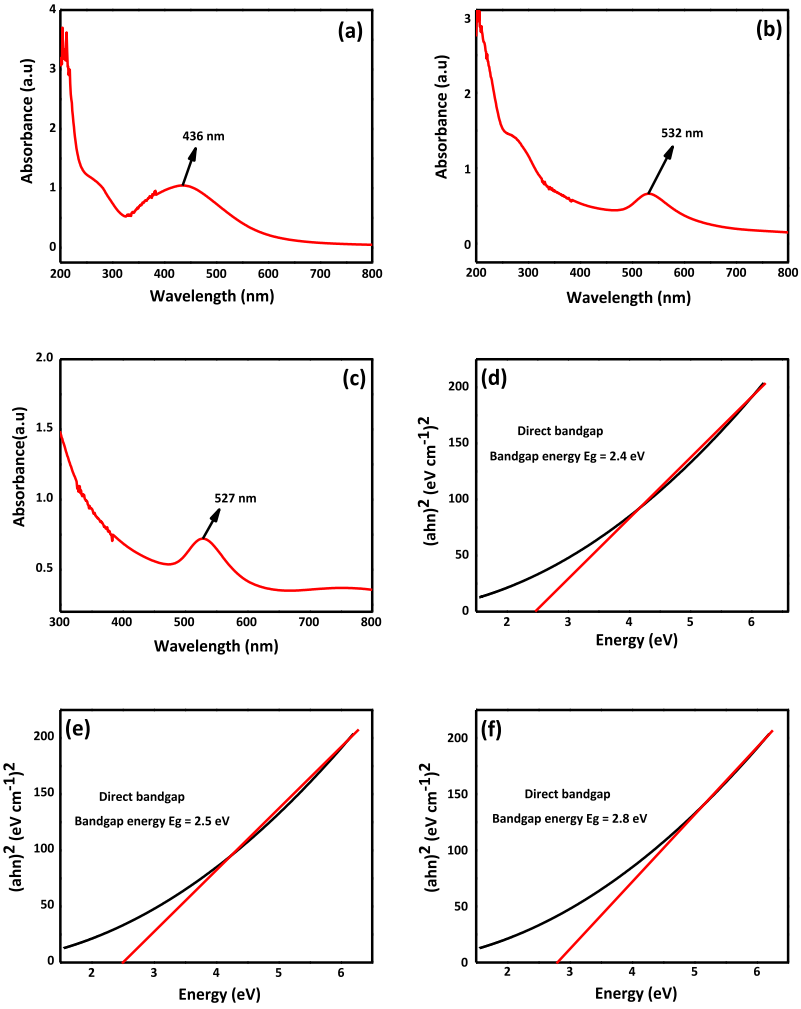

Fig. 6. (a = AgNPs, b = AuNPs, c = Ag/Au BNPs) UV–visible Spectrum and (d–f) Tauc plots of Ag, Au and Ag/Au BNPs.

shown in Fig. 4a. Total polyphenols were determined by using straight line equation where $y = 8.76x + 0.128$. In this equation y is the absorbance of the samples (bark extract) taken in triplicate as shown in Fig. 3b and x is the number of polyphenolic compounds. The average absorbance of the bark extract at 740 nm was taken and put in the equation. The content of total polyphenols after calculation

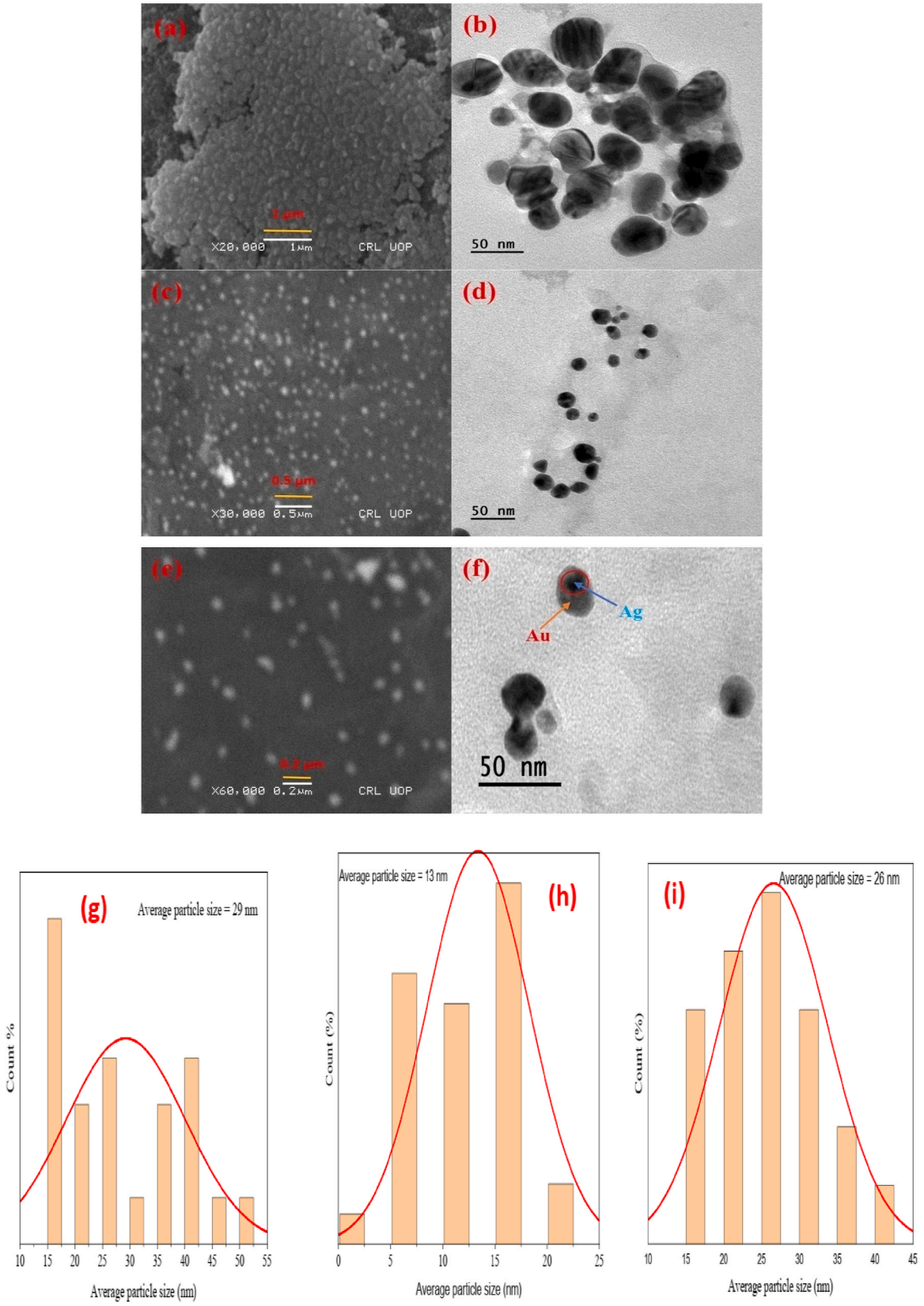

Fig. 7. SEM (a, c, and f) and TEM (b, d, and f) images and size distribution (g, h and i) of AgNPs, AuNPs, and Ag/Au BNPs.

was found as 0.0362 mg/mg of the dried bark extract.

3.2. Determination of total flavonoid compounds

Method of Chang et al., was followed to measure total flavonoids content in the bark extract of T.A (Table 2). A five point calibration curve was plotted with R^2 value as 0.9875 as shown in Fig. 4b.Using straight line equation (y = 6.222x – 0.014) the flavonoids content in bark extract was found as 0.2928 mg/mg of the dried extract. Absorbance was found at 415 nm.

3.3. FTIR analysis

FT-IR examination for the prepared NPs was carried out via FTIR (500-4000 cm^{-1}) where solid NPs powder was introduced. The FTIR results for prepared NPs are indicated in Fig. 5 where **5(a)** shows result of the AgNPs. The band at 571 cm^{-1} is because of the AgNPs. Groove showed at 820 cm^{-1} is due to aromatic C-H vibration because of the free catechins which further reveals some polyphenol moieties (having at least one aromatic ring) in combination with AgNPs. Peak at 1051 cm^{-1} is of C-N, the aliphatic amine. Band corresponding to 1646 cm^{-1} is due to C = O functional group of polyphenols, such as catechin gallate, epicatechin gallate and the aflavins. The peak at 3489 cm^{-1} is due to the OH group of flavonoids and tannin moieties. Similarly, Fig. 5b, indicates the FTIR result of AuNPs, the band observed at 456 cm^{-1} is because of the biologically synthesized AuNPs. Peaks at 1022 cm^{-1} refers to C-N vibration and groove at 1227 $cm^{-1}$is because of N-O symmetric stretching of the compounds of N-O nitro. Bands at 1627 cm^{-1} and 1732 cm^{-1} corresponds to carbonyl (C = O) stretching of aldehydes, ketones, and carboxylic acid in the biologically synthesized nanoparticles. Band at 2922 cm^{-1} refers to the C-H group. Band at 3307 cm^{-1} corresponds to OH functional group of the phenol. Finally, Fig. 5c, shows the FTIR result of Ag/Au BNPs. Grooves at 418 cm^{-1} and 552 cm^{-1} refers to Ag and Au NPs respectively. Band at 1637 cm^{-1} is due to the binding of the (NH)C = O group with the NPs. Peak at 3326 cm^{-1} is because of the phenolic hydroxyl (OH) associated with flavonoids and tannin moieties. The above results clearly confirmed the successful biogenic synthesis of the AgNPs, AuNPs and Ag/Au bimetallic BNPs.

3.4. Analysis of UV and Band gap energy

The UV characterization of the prepared NPs (Ag, Au and Ag/Au) was performed by dispersing them in ethanol solvent employing UV–visible Spectrophotometer in 200–800 nm wavelength range. The peaks observed at 436 nm, 532 nm and 527 nm corresponds to AgNPs, AuNPs, and Ag/Au BNPs respectively as revealed in Fig. 6 (a,b,c). The nanoparticles' band gap energies were calculated using Tauc plot equation:

$$(\alpha h\upsilon)^{\gamma} = A(h\upsilon - Eg) \quad (5)$$

Here α = absorption coefficient, h = planks constant, υ = photons frequency, A = proportionality constant, Eg = Bandgap energy, γ = electronic transition.

Which is either as 2, 1/2, 2/3, or 1/3, depends on the environment. Fig. 6 (d,e,f) shows Tauc plots for all the synthesized NPs. A straight line was obtained when we plotted $(\alpha h\nu)^2$ versus (hν), which further explained that the absorption edge was caused by an indirect allowed transition (n = 1 for a direct allowed transition). Optical band gap (Eg) corresponds to intercept of straight line. Direct band gap energy of the AgNPs, AuNPs and Ag/Au BNPs is Eg = 2.4 eV, Eg = 2.5 eV, and Eg = 2.8 eV, respectively. The band gap energies reported by others researchers for AgNPs are: 2.20 eV, 2.16 eV, 2.12 eV, 2.11 eV and 1.84 eV, 3.4 eV [43], 2.28 eV [44], 2.5 eV [45], 3.39eV [46]. Previously reported band gap energies for AuNPs are 3.41 Ev, 2.95 and 2.90 [47], 2.08 eV, 2.13, 3.53eV [48], 4.55eV [49] and 2.50–2.70 eV [50], 3.5 eV [51], 3.87eV [52] for Ag/Au BNPs. These results clearly indicated strong agreement between the previous literature and our synthesized NPs confirming thriving fabrication of the Ag, Au and Ag/Au BNPs. Higher band gap energy of Ag/Au composite relative to individual components Ag and Au shows smaller particles of the synthesized NPs. Moreover, the variations in the band gap energies of Ag, Au and Ag/Au BNPs with reported literature may be due to the size and quantum effects, composition, crystal structure, surface effects, plasmonic resonances, alloying and doping, synthesis methods etc.

3.5. SEM and TEM analysis

For the study of morphology of the synthesized NPs,SEM and TEM were used. The SEM and TEM results of synthesized Ag, Au and Ag/Au bimetallic NPs are indicated in Fig. 7(a–c and e) and Fig. 7(b–d and f) respectively. Fig. 7 (a) shows the SEM result of AgNPs which clearly shows that AgNPs are spherical and oval shaped and homogeneously distributed. Fig. 7 (c) shows SEM result of the AuNPs which are uniformly distributed and spherical. Finally, Fig. 7 (e & f), shows the homogeneous, uniform distribution of the AgNPs in the AuNPs. Furthermore, it also indicates that the spherical AgNPs are surrounded by the AuNPs, where AgNPs act as core and the AuNPs as shell, confirming successful fabrication of Ag/Au BNPs. Similarly, the TEM result for the synthesized NPs in Fig. 7 (b–d and f), clearly shows that all the synthesized NPs are in the nano range. The results clearly indicate the successful fabrication of the synthesized NPs. Finally, Fig. 7 (g, h & i) indicate the particle size distributions of AgNPs, AuNPs, and Ag/Au BNPs respectively. These histograms clearly show the average particles size of all the synthesized NPs which is 29 nm (AgNPs), 13 nm (AuNPs) and 26 nm (Ag/Au BNPs). The difference in the size of the synthesized NPs is may be due to the synthesis strategies, reduction potentials, crystal structure, surface energies, seed-mediated growth (for Ag/Au BNPs), alloying effects (for Ag/Au BNPs), stabilizers and capping agents,

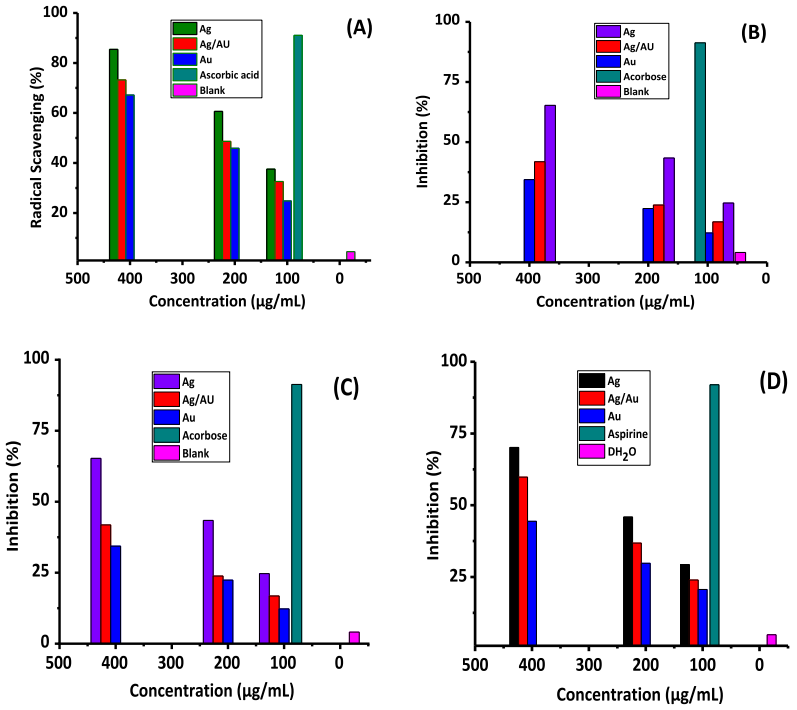

Fig. 8. (A) Antioxidant, (B) Alpha Amylase, (C) Alpha-glucosidase inhibition and (D) Anti-inflammatory (HRBCs heat induced hemolysis) activities.

reaction kinetics, aggregation, and ostwald ripening etc (see Table 2).

3.6. Bio potential of AgNPs, AuNPs and Ag/Au BNPs

3.6.1. Antioxidant activity

The antioxidant potential of the green synthesized AgNPs, AuNPs and Ag/Au BNPs were tested against the standard ascorbic acid [41]. It is obvious from the results as mentioned in Fig. 8 (a) and Table 3 that AgNPs showed the highest antioxidant activity of 85 % at 400 µg/ml, followed by Ag/Au BNPs 72 % and AuNPs 67 % in dose dependent manner at three different concentrations i.e.100 µg/mL > 200 µg/mL > 400 µg/mL respectively with the effective IC_{50} values around 160, 222 and 263 µg/ml while the lowest activity was recorded for AgNPs 37 %, Ag/Au BNPs 31 % and AuNPs 24 % at 100 µg/ml, which demonstrates its dosage based mechanism. In previous studies nanoparticles' antioxidant property is a well-known phenomenon as it donates an electron to the free radicals, which neutralizes the free radicals to limit cell damage through oxidative stress [53]. Furthermore, studies on green synthesized AgNPs using *Cestrum nocturnum* plant extract as a reducing agent showed robust antioxidant activity with reference to standard ascorbic acid [54]. In a published literature bimetallic Ag-ZnO nano-composites demonstrated higher effectiveness in contrast to silver NPs alone [55]. Similarly green synthesized AuNPs from grapefruit peel extract possess effective free radicals scavenging active in DPPH antioxidant assay against ascorbic acid [56] but in our results lowest antioxidant efficacy of AuNPs observed which was may be due to their size, nature of bonding and morphology and there bio-compatibility with the plant extract.

3.6.2. Alpha amylase inhibition activity

The alpha amylase inhibition of green synthesized AgNPs, AuNPs and Ag/Au BNPs was performed according to the published procedure [42], against standard anti-diabetic drug acarbose. From our findings as mentioned in Fig. 8 (b) and Table 3, the peak activity at 400 µg/mL i.e. AgNPs 64 %, Ag/Au BNPs 41 % and AuNPs 34 % with effective IC_{50} values of 275, 500 and 600 µg/mL at various doses i.e. 100 µg/mL > 200 µg/mL > 400 µg/mL but with decreasing NPs concentration its activity gradually reduced such as i. e. 24 %, 16 % and 12 % at 100 µg/mL respectively and this trend is quite consistent with the previous scientific literatures [57,58]. The Ag/Au NPswere noticed to have an intermediate antiplasmodial potential as compared to Ag and Au alone, it may be due to balancing effect between the two elements during bonding or may be interaction between the enzyme's active site with the nanocomposites. Results derived from this study are comparatively similar with the reported data [42,59].

3.6.3. Alpha-glucosidase inhibition activity

Diabetes can be managed by obstructing the carbohydrates digestive enzymes to maintain steady glycaemic index. Alpha-glucosidase inhibition of green synthesized AgNPs, AuNPs and Ag/Au BNPs were assessed by following optimized protocols [41]

Table 3
Summary of different biological activities exhibited by AgNPs, AuNPs and Ag/Au BNPs.

(A). Antioxidant Activity			
Sample	Concentration (μg/mL)	% Activity	IC_{50}μg/mL
Standard (Ascorbic acid)	100		
AgNPs	100	37	160.9191
-do-	200	60	
-do-	400	85	
Ag/Au BNPs	100	31	222.3037
-do-	200	48	
-do-	400	72	
AuNPs	100	24	263.1131
-do-	200	45	
-do-	400	67	
(B). Alpha Amylase Inhibition Activity			
Standard (Acarbose)	**Concentration (μg/mL)**	**% Activity**	**IC_{50}μg/mL**
AgNPs	100	24	275.4138
-do-	200	43	
-do-	400	64	
Ag/Au BNPs	100	16	500.4947
-do-	200	23	
-do-	400	41	
AuNPs	100	12	609.3677
-do-	200	22	
-do-	400	34	
(C). Alpha Glucosidase Inhibition Activity			
Standard (Acarbose)	100	**% Activity**	**IC_{50}μg/mL**
AgNPs	100	25	309.156
-do-	200	37	
-do-	400	59	
Ag/Au BNPs	100	20	412.1117
-do-	200	31	
-do-	400	48	
AuNPs	100	11	491.0278
-do-	200	24	
-do-	400	40	
(D). HRBCs Heat Induced Hemolysis Activity			
Standard (Aspirin)	100	**% Activity**	**IC_{50}μg/mL**
AgNPs	100	28	245.209
-do-	200	45	
-do-	400	69	
Ag/Au NPs	100	23	316.1331
-do-	200	36	
-do-	400	59	
AuNPs	100	20	468.5185
-do-	200	29	
-do-	400	43	

against the standard antidiabetic drug acarbose at various concentrations of NPs such as 100 μg/mL, 200 μg/mL and 400 μg/mL. The results indicated in Fig. 8 (c) and Table 3 shows that the alpha-amylase inhibitory potential of AgNPs, Ag/Au BNPs and AuNPs gradually increases with increasing concentration like at 100 μg/mL i.e. Ag 25 %, Ag/Au 20 %, and Au 11 % respectively, but the highest activity was observed at 400 μg/mL i.e. AgNPs 59 %, Ag/Au BNPs 48 %, and AuNPs 40 % with IC_{50} values as 309, 412 and 491 μg/mL respectively. Carbohydrates active enzymes inhibition through green synthesis NPs and BNPs in a dose depended manner are quiet parallel with previous manuscripts [60]. Moreover in our results the Ag/Au BNPs have a stable intermediate alpha-glucosidase inhibitory activity as mentioned in earlier reports [61,62]. Hence making it as an alternative option for treating or managing diabetes mellitus, but some of the possible toxicities are associated with BNPs which needs to be addressed in future studies [63].

3.6.4. HRBCs heat induced hemolysis activity

The anti-inflammatory potential of green synthesized AgNPs, AuNPs and Ag/Au BNPs was performed by HRBCs heat induced hemolysis assay against the standard anti-inflammatory drug aspirin at various concentrations i.e. 100 μg/mL, 200 μg/mL and 400 μg/mL. The results mentioned in Fig. 8 (d) and Table 3 indicates that the NPs protection of the human red bloods cells from hemolysis was highest at 400 μg/mL such as AgNPs 69 %, Ag/Au BNPs 59 % and AuNPs 43 % with IC_{50} values of 245, 316 and 468 μg/mL but drastically falls with the reducing concentrations such as at 100 μg/mL i.e. AgNPs 28 %, Ag/Au BNPs 23 % and AuNPs 20 %, with reference to published reports which is clearly a concentration-dependent effect [64]. However the Ag/Au BNPs gives a balance

Table 4
Comparison between current and previously published results.

S.No	Name of the activity	Type of Nanoparticle	Present Study (Percentage inhibition)	Previous Published results	References
1	Antioxidant activity	AgNPs	37 %	57 %	[68]
		AuNPs	24 %	59 %	
		Ag/Au BNPs	31 %	63 %	
2	Alpha amylase inhibition activity	AgNPs	64 %	55 %	[69,70],
		AuNPs	34 %	86 %, 78 %	[42]
		Ag/Au BNPs	41 %	26 %	
3	Alpha glucosidase inhibition activity	AgNPs	59 %	47 %	[69,70],
		AuNPs	40 %	71 %	[42]
		Ag/Au BNPs	48 %	41 %	
4	HRBCs heat induced hemolysis activity	AgNPs	28 %	73 %	[71,72]
		AuNPs	20 %	94 %	

anti-inflammatory activity, which is lower than AgNPs but greater than AuNPs which is perhaps due to redox activity, enzyme specificity, particle geometry, biocompatibility and cytotoxicity [65–67].

Table 4 shows that the percent inhibition for antioxidant activity in published reports which is a bit high then our work with inhibition for Ag/Au BNPs as the highest followed by AuNPs and then AgNPs which is in contrast to our results where AgNPs have the highest inhibition and AuNPs have the lowest. If we look for μ-amylase results in previously published work, AuNPs have the highest efficiency followed by AgNPs. These results are also a bit high from our ones and same in case of μ-glucosidase and HRBCs hemolysis activity. This difference in results is because of the plants previous researchers have used for green synthesis of NPs because every plant has different kinds and abundance of phytochemicals which are responsible for reduction and capping of NPs. Plants which have great capping ability results in very much stable NPs and hence NPs' potential efficacy in every field increases.

4. Conclusion

Nanoparticles of Ag, Au and bimetallic Ag/Au were successfully prepared through green synthesis process by utilizing T.A bark extract as a reducing and capping agent. The determination of total polyphenols and flavonoids in this research is a proof of the reducing ability of bark extract. The nanoparticles were synthesized within 10 min and UV, FTIR confirmed the initial formation while the size and morphology were confirmed through SEM and TEM. The particles synthesized in this short span of time and no harmful reaction waste had a size of 29 nm, 13 nm and 26 nm for AgNPs, AuNPs and Ag/Au BNPs respectively. Our research also confirmed the great inhibition activities of the synthesized NPs where AgNPs stood tall among all NPs with highest percent inhibition at all concentrations. Based upon our research findings these nanoparticles offer new avenues for utilizing them as a novel nano therapy against oxidative stress, inflammation and diabetes etc. Furthermore these findings needs to be thoroughly evaluated in *in-vivo* experimentation in order to address its toxicities associated with its administration as nanomedicine.

Data availability statement

This research study is a new work for PhD research and not publishes yet so the data will be made available on turnitin repository after thesis submission.

CRediT authorship contribution statement

Sumbul Mujahid: Methodology, Investigation, Funding acquisition. **Nida Ambreen:** Writing – review & editing, Supervision. **Muhammad Yaseen:** Validation. **Muhammad Ihtesham:** Data curation. **Khalid Mohammed Khan:** Project administration. **Muhammad Nasimullah Qureshi:** Validation.

Declaration of competing interest

The authors declare that they have no known competing financial interests or personal relationships that could have appeared to influence the work reported in this paper.

Acknowledgements

Miss Sumbul Mujahid (Pin # 2BS3097) acknowledges Higher Education Commission of Pakistan for the financial support through the award of HEC Indigenous 5000 PhD fellowship (Phase II Batch III).

References

[1] M. Yaseen, A. Khan, M. Bououdina, S.Q. Shah, A.F. Alanazi, Z.A. Khattak, W. Hussain, S. Bibi, S. Ahmad, A. Hameed, Fabrication, characterization, photocatalytic and biological performances of Mn/ZnO–SiO2 and ZnO–SiO2/PVA based ternary nanocomposites, Z. Phys. Chem. (0) (2024), https://doi.org/10.1515/zpch-2023-0423.

[2] A. Khan, M. Ullah, M. Humayun, N. Shah, B.P. Chang, M. Yaseen, Preparation and functionalization of zinc oxide nanoparticles with polymer microgels for potential catalytic applications, J Disper Sci Technol 43 (2) (2022) 259–272, https://doi.org/10.1080/01932691.2020.1839481.

[3] S. Pittarate, J. Rajula, A. Rahman, P. Vivekanandhan, M. Thungrabeab, S. Mekchay, P. Krutmuang, Insecticidal effect of zinc oxide nanoparticles against Spodoptera frugiperda under laboratory conditions, J. Insects 12 (11) (2021) 1017, https://doi.org/10.3390/insects12111017.

[4] a) A. Rahman, S. Pittarate, V. Perumal, J. Rajula, M. Thungrabeab, S. Mekchay, P. Krutmuang, Larvicidal and antifeedant effects of copper nano-pesticides against Spodoptera frugiperda (JE Smith) and its immunological response, J. Insects 13 (11) (2022) 1030, https://doi.org/10.3390/insects13111030;
b) M.C. Nadia, L. Eric, T. Gianggiacomo, C. Gregorio, Applications of chitosan in food, pharmaceuticals, medicine, cosmetics, agriculture, textiles, pulp and paper, biotechnology, and environmental chemistry, Env. Chem. Lett. 17 (2019) 1667.

[5] S.J. Nadaf, N.R. Jadhav, H.S. Naikwadi, P.L. Savekar, I.D. Sapkal, M.M. Kambli, I.A. Desai, Green synthesis of gold and silver nanoparticles: updates on research, patents, and future prospects, OpenNano 8 (2022) 100076, https://doi.org/10.1016/j.onano.2022.100076.

[6] P. Vivekanandhan, S. Deepa, E.J. Kweka, M.S. Shivakumar, Toxicity of Fusarium oxysporum-VKFO-01 derived silver nanoparticles as potential inseciticide against three mosquito vector species (Diptera: Culicidae), J. Clust. Sci. 29 (2018) 1139–1149, https://doi.org/10.1007/s10876-018-1423-1.

[7] Kalaimurugan D, P. Vivekanandhan, P. Sivasankar, K. Durairaj, P. Senthilkumar, M.S. Shivakumar, S. Venkatesan, Larvicidal activity of silver nanoparticles synthesized by Pseudomonas fluorescens YPS3 isolated from the Eastern Ghats of India, J. Clust. Sci 30 (2019) 225–233, https://doi.org/10.1007/s10876-018-1478-z.

[8] P. Vivekanandhan, S. Panikar, V. Sethuraman, A. Usha-Raja-Nanthini, M.S. Shivakumar, Toxic and synergetic effect of plant essential oils along with nano-emulsion for control of three mosquito species, J Nat Pestic Res 5 (2023) 100045, https://doi.org/10.1016/j.napere.2023.100045.

[9] R. Chinnasamy, K. Chinnaperumal, T. Cherian, K. Thamilchelvan, B. Govindasamy, C. Vetrivel, V. Perumal, P. Willie, P. Krutmuang, Eco-friendly phytofabrication of silver nanoparticles using aqueous extract of Aristolochia bracteolata Lam: its antioxidant potential, antibacterial activities against clinical pathogens and malarial larvicidal effects, Biomass Convers Biorefin (2023) 1–16, https://doi.org/10.1007/s13399-023-03750-8.

[10] O.S. ElMitwalli, O.A. Barakat, R.M. Daoud, S. Akhtar, F.Z. Henari, Green synthesis of gold nanoparticles using cinnamon bark extract, characterization, and fluorescence activity in Au/eosin Y assemblies, J Nanopart Res 22 (2020) 1–9, https://doi.org/10.1007/s11051-020-04983-8.

[11] C. Botteon, L. Silva, G. Ccana-Ccapatinta, T. Silva, S. Ambrosio, R. Veneziani, J. Bastos, P. Marcato, Biosynthesis and characterization of gold nanoparticles using Brazilian red propolis and evaluation of its antimicrobial and anticancer activities, Sci. Rep. 11 (1) (2021) 1974, https://doi.org/10.1038/s41598-021-81281-w.

[12] S. Balasubramanian, S.M.J. Kala, T.L. Pushparaj, Biogenic synthesis of gold nanoparticles using Jasminum auriculatum leaf extract and their catalytic, antimicrobial and anticancer activities, J. Drug Deliv. Sci. Technol. 57 (2020) 101620, https://doi.org/10.1016/j.jddst.2020.101620.

[13] H. Lu, X. Zhang, S.A. Khan, W. Li, L. Wan, Biogenic synthesis of MnO2 nanoparticles with leaf extract of Viola betonicifolia for enhanced antioxidant, antimicrobial, cytotoxic, and biocompatible applications, Front. Microbiol. 12 (2021) 761084, https://doi.org/10.3389/fmicb.2021.761084.

[14] D. Sharma, S. Kanchi, K. Bisetty, Biogenic synthesis of nanoparticles: a review, Arab. J. Chem. 12 (8) (2019) 3576–3600, https://doi.org/10.1016/j.arabjc.2015.11.002.

[15] M. Ndikau, N.M. Noah, D.M. Andala, E. Masika, Green synthesis and characterization of silver nanoparticles using Citrullus lanatus fruit rind extract, Int J Anal Chem (2017), https://doi.org/10.1155/2017/8108504.

[16] T.-T. Vo, C.-H. Dang, V.-D. Doan, V.-S. Dang, T.-D. Nguyen, Biogenic synthesis of silver and gold nanoparticles from Lactuca indica leaf extract and their application in catalytic degradation of toxic compounds, J. Inorg. Organomet. Polym. Mater. 30 (2020) 388–399, https://doi.org/10.1007/s10904-019-01197-x.

[17] P. Dube, S. Meyer, A. Madiehe, M. Meyer, Antibacterial activity of biogenic silver and gold nanoparticles synthesized from Salvia africana-lutea and Sutherlandia frutescens, Nanotechnol 31 (50) (2020) 505607, https://doi.org/10.1088/1361-6528/abb6a8.

[18] P. Singh, Y.J. Kim, C. Wang, R. Mathiyalagan, M. El-Agamy Farh, D.C. Yang, Biogenic silver and gold nanoparticles synthesized using red ginseng root extract, and their applications, Artif. Cells, Nanomed. Biotechnol. 44 (3) (2016) 811–816, https://doi.org/10.3109/21691401.2015.1008514.

[19] S. Bhakya, S. Muthukrishnan, M. Sukumaran, M. Muthukumar, Biogenic synthesis of silver nanoparticles and their antioxidant and antibacterial activity, Appl. Nanosci. 6 (2016) 755–766, https://doi.org/10.1007/s13204-015-0473-z.

[20] B.H. Abbasi, M. Zaka, S.S. Hashmi, Z. Khan, Biogenic synthesis of Au, Ag and Au–Ag alloy nanoparticles using Cannabis sativa leaf extract, IET Nanobiotechnol. 12 (3) (2018) 277–284, https://doi.org/10.1049/iet-nbt.2017.0169.

[21] A. Mahfoudhi, F.P. Prencipe, Z. Mighri, F. Pellati, Metabolite profiling of polyphenols in the Tunisian plant Tamarix aphylla (L.) Karst, J. Pharm. Biomed. Anal. 99 (2014) 97–105, https://doi.org/10.1016/j.jpba.2014.07.013.

[22] A.M. Souliman, H.H. Barakat, A.M. El-Mousallamy, M.S. Marzouk, M.A. Nawwar, Phenolics from the bark ofTamarix aphylla, Phytochem 30 (11) (1991) 3763–3766, https://doi.org/10.1016/0031-9422(91)80105-A.

[23] S. Ismaeel, H. Jaber, R. Zayed, Isolation of β-sitosterol from Tamarix aphylla of Iraq, Biochem. Cell. Arch. 20 (2) (2020). https://connectjournals.com/03896.2020.20.6497.

[24] S.A. Alrumman, Phytochemical and antimicrobial properties of Tamarix aphylla L. leaves growing naturally in the Abha Region, Saudi Arabia, Arab J Sci Eng 41 (2016) 2123–2129, https://doi.org/10.1007/s13369-015-1900-x.

[25] R. Gul, M. Saddique, M.A. Khan, D. Khan, S. Tabassum, K.U. Rehman, Eco-friendly synthesis of silver nanoparticles and its biological evaluation using Tamarix aphylla leaves extract, Mater. Technol. 37 (9) (2022) 962–969, https://doi.org/10.1080/10667857.2021.1908770.

[26] M.A. Orabi, M.M. Salem-Bekhit, E.I. Taha, E.-S. Abdel-Sattar, O.S. Alqahtani, F.A. Al-Joufi, B.A. Abdel-Wahab, A.M. Alshabi, H.S. Alyami, J. Ahmad, Design, characterization, and antimicrobial evaluation of copper nanoparticles utilizing tamarixinin a ellagitannin from galls of Tamarix aphylla, Pharmaceuticals 15 (2) (2022) 216, https://doi.org/10.3390/ph15020216.

[27] I.H. Shah, M. Ashraf, A.R. Khan, M.A. Manzoor, K. Hayat, S. Arif, I.A. Sabir, M. Abdullah, Q. Niu, Y. Zhang, Controllable synthesis and stabilization of Tamarix aphylla-mediated copper oxide nanoparticles for the management of Fusarium wilt on musk melon, 3 Biotech 12 (6) (2022) 128, https://doi.org/10.1007/s13205-022-03189-0.

[28] M.S. Alwhibi, K.M. Ortashi, A.A. Hendi, M. Awad, D.A. Soliman, M. El-Zaidy, Green synthesis, characterization and biomedical potential of Ag@ Au core–shell noble metal nanoparticles, J. King Saud Univ. Sci. 34 (4) (2022) 102000, https://doi.org/10.1016/j.jksus.2022.102000.

[29] S. Ganaie, T. Abbasi, S. Abbasi, Rapid and green synthesis of bimetallic Au–Ag nanoparticles using an otherwise worthless weed Antigonon leptopus, J. Exp. Nanosci. 11 (6) (2016) 395–417, https://doi.org/10.1080/17458080.2015.1070311.

[30] M. Yaseen, M. Humayun, A. Khan, M. Idrees, N. Shah, S. Bibi, Photo-assisted removal of rhodamine B and nile blue dyes from water using CuO–SiO2 composite, Molecules 27 (16) (2022) 5343, https://doi.org/10.3390/molecules27165343.

[31] A. Ahmad, F. Syed, A. Shah, Z. Khan, K. Tahir, A.U. Khan, Q. Yuan, Silver and gold nanoparticles from Sargentodoxa cuneata: synthesis, characterization and antileishmanial activity, Rsc Adv 5 (90) (2015) 73793–73806, https://doi.org/10.1039/C5RA13206A.

[32] A.A. Hendi, M.A. Awad, M.M. Alanazi, P. Virk, A.W. Alrowaily, T. Bahlool, N.M. Merghan, F. Aouaini, B. Hagmusa, Phytomediated synthesis of bimetallic Ag/Au nanoparticles using orange peel extract and assessment of their antibacterial and anitcancer potential, J. King Saud Univ. Sci. 35 (2) (2023) 102510, https://doi.org/10.1016/j.jksus.2022.102510.

[33] M. Szymanski, R. Dobrucka, Evaluation of phytotoxicity of bimetallic Ag/Au nanoparticles synthesized using Geum urbanum L, J. Inorg. Organomet. Polym. Mater. 31 (2021) 2459–2470, https://doi.org/10.1007/s10904-020-01814-0.

[34] N. Rezk, A.S. Abdelsattar, S. Makky, A.H. Hussein, A.G. Kamel, A. El-Shibiny, New formula of the green synthesised Au@ Ag core@ shell nanoparticles using propolis extract presented high antibacterial and anticancer activity, AMB Expr 12 (1) (2022) 1–14, https://doi.org/10.1186/s13568-022-01450-6.

[35] A. Lagashetty, S.K. Ganiger, Synthesis, characterization and antibacterial study of Ag–Au Bi-metallic nanocomposite by bioreduction using piper betle leaf extract, Heliyon 5 (12) (2019) e02794, https://doi.org/10.1016/j.heliyon.2019.e02794.
[36] J.M.A. Villalobos-Noriega, E. Rodríguez-León, C. Rodríguez-Beas, E. Larios-Rodríguez, M. Plascencia-Jatomea, A. Martínez-Higuera, H. Acuña-Campa, A. García-Galaz, R. Mora-Monroy, F.J. Alvarez-Cirerol, Au@ Ag Core@ Shell nanoparticles synthesized with Rumex hymenosepalus as antimicrobial agent, Nanosc Res Lett 16 (2021) 1–19, https://doi.org/10.1186/s11671-021-03572-5.
[37] M.A. Nawwar, S. Hussein, N. Ayoub, K. Hofmann, M. Linscheid, M. Harms, K. Wende, U. Lindequist, Aphyllin, the first isoferulic acid glycoside and other phenolics from Tamarix aphylla flowers, Pharmazie 64 (5) (2009) 342–347, https://doi.org/10.1691/ph.2009.8822.
[38] A. Iqbal, I. Siraj-ud-Din, G. Ali, Z.U. Rahman, F. Rabi, M.S. Khan, Pharmacological evaluation of Tamarix aphylla for Anti-inflammatory, anti-pyretic and anti-nociceptive activities in Standard Animal models, West Ind Med J (2017) 1–22.
[39] L. Jiang, S. Numonov, K. Bobakulov, M.N. Qureshi, H. Zhao, H.A. Aisa, Phytochemical profiling and evaluation of pharmacological activities of Hypericum scabrum L, Molecules 20 (6) (2015) 11257–11271, https://doi.org/10.3390/molecules200611257.
[40] C.-C. Chang, M.-H. Yang, H.-M. Wen, J.-C. Chern, Estimation of total flavonoid content in propolis by two complementary colorimetric methods, J. Food Drug Anal. 10 (3) (2002), https://doi.org/10.38212/2224-6614.2748.
[41] K. Dybka-Stepien, A. Otlewska, P. Góźdź, M. Piotrowska, The renaissance of plant mucilage in health promotion and industrial applications: a review, Nutrients 13 (10) (2021) 3354, https://doi.org/10.3390/nu13103354.
[42] S. Anjum, K. Nawaz, B. Ahmad, C. Hano, B.H. Abbasi, Green synthesis of biocompatible core–shell (Au–Ag) and hybrid (Au–ZnO and Ag–ZnO) bimetallic nanoparticles and evaluation of their potential antibacterial, antidiabetic, antiglycation and anticancer activities, RSC Adv. 12 (37) (2022) 23845–23859, https://doi.org/10.1039/D2RA03196E.
[43] A. Das, R. Kumar, S. Goutam, S. Sagar, Sunlight irradiation induced synthesis of silver nanoparticles using glycolipid bio-surfactant and exploring the antibacterial activity, J. Bioeng Biomed. Sci. 6 (5) (2016). https://10.4172/2155-9538.1000208.
[44] J. Joy, M.S. Gurumurthy, R. Thomas, M. Balachandran, Biosynthesized Ag nanoparticles: a promising pathway for bandgap tailoring, Biointerface Res. Appl. Chem. 11 (2) (2021) 8875–8883, https://doi.org/10.33263/BRIAC112.88758883.
[45] A. Aziz, M. Khalid, M.S. Akhtar, M. Nadeem, Z. Gilani, H.U.H.K. Asghar, J. Rehman, Z. Ullah, M. Saleem, Structural, morphological and optical investigations of silver nanoparticles synthesized by sol-gel auto-combustion method, Dig. J. Nanomater. Biostruct. 13 (3) (2018), https://doi.org/10.1016/j.inoche.2022.109532.
[46] I.A.M. Ali, A.B. Ahmed, H.I. Al-Ahmed, Green synthesis and characterization of silver nanoparticles for reducing the damage to sperm parameters in diabetic compared to metformin, Sci. Rep. 13 (1) (2023) 2256, https://doi.org/10.1038/s41598-023-29412-3.
[47] A. Dey, A. Yogamoorthy, S. Sundarapandian, Green synthesis of gold nanoparticles and evaluation of its cytotoxic property against colon cancer cell line, Res. J. Life Sci. Bioinform. Pharm. Chem. Sci 4 (2018) 1–17. https://10.26479/2018.0406.01.
[48] J.S. Boruah, C. Devi, U. Hazarika, P.V.B. Reddy, D. Chowdhury, M. Barthakur, P. Kalita, Green synthesis of gold nanoparticles using an antiepileptic plant extract: in vitro biological and photo-catalytic activities, RSC Adv. 11 (45) (2021) 28029–28041, https://doi.org/10.1039/D1RA02669K.
[49] N. Singh, M.K. Das, A. Ansari, D. Mohanta, P. Rajamani, Biogenic nanosized gold particles: physico-chemical characterization and its anticancer response against breast cancer, Biotechnol. Rep 30 (2021) e00612, https://doi.org/10.1016/j.btre.2021.e00612.
[50] S. AdibAmini, A.H. Sari, D. Dorranian, Optical properties of synthesized Au/Ag Nanoparticles using 532 nm and 1064 nm pulsed laser ablation: effect of solution concentration, SN Appl. Sci. 5 (4) (2023) 122, https://doi.org/10.1007/s42452-023-05310-1.
[51] N.K. Abdalameer, K.A. Khalaph, E.M. Ali, Ag/AgO nanoparticles: green synthesis and investigation of their bacterial inhibition effects, Mater Today: Proc 45 (2021) 5788–5792, https://doi.org/10.1016/j.matpr.2021.03.166.
[52] S.A. Shah, K.-J. Hu, M. Naveed, S.N.A. Shah, S. Hu, S. Lu, F. Song, Synthesis of Au doped Ag nanoclusters and the doping effect of Au atoms on their physical and optical properties, Mater. Res. Express 7 (1) (2019) 016506. https://10.1088/2053-1591/ab5bde.
[53] A.V. Samrot, S.P. Ram Singh, R. Deenadhayalan, V.V. Rajesh, S. Padmanaban, K. Radhakrishnan, Nanoparticles, a double-edged sword with oxidant as well as antioxidant properties—a review, Oxygen 2 (4) (2022) 591–604, https://doi.org/10.3390/oxygen2040039.
[54] A.K. Keshari, R. Srivastava, P. Singh, V.B. Yadav, G. Nath, Antioxidant and antibacterial activity of silver nanoparticles synthesized by Cestrum nocturnum, J. Ayurveda Integr. Med. 11 (1) (2020) 37–44, https://doi.org/10.1016/j.jaim.2017.11.003.
[55] M. Bagheri, M. Validi, A. Gholipour, P. Makvandi, E. Sharifi, Chitosan nanofiber biocomposites for potential wound healing applications: antioxidant activity with synergic antibacterial effect, Bioeng. Transl Med 7 (1) (2022) e10254, https://doi.org/10.1002/btm2.10254.
[56] K.A. Bokhary, F. Maqsood, M. Amina, A. Aldarwesh, H.K. Mofty, H.M. Al-Yousef, Grapefruit extract-mediated fabrication of photosensitive aluminum oxide nanoparticle and their antioxidant and anti-inflammatory potential, Nanomaterials 12 (11) (2022) 1885, https://doi.org/10.3390/nano12111885.
[57] K. Balan, W. Qing, Y. Wang, X. Liu, T. Palvannan, Y. Wang, F. Ma, Y. Zhang, Antidiabetic activity of silver nanoparticles from green synthesis using Lonicera japonica leaf extract, RSC Adv. 6 (46) (2016) 40162–40168, https://doi.org/10.1039/C5RA24391B.
[58] Jini D, S. Sharmila, Green synthesis of silver nanoparticles from Allium cepa and its in vitro antidiabetic activity, Mater. Today: Proc 22 (2020) 432–438, https://doi.org/10.1016/j.matpr.2019.07.672.
[59] I. Saikia, M. Hazarika, S. Yunus, M. Pal, M.R. Das, J.C. Borah, C. Tamuly, Green synthesis of Au-Ag-In-rGO nanocomposites and its α-glucosidase inhibition and cytotoxicity effects, Mater. Lett. 211 (2018) 48–50, https://doi.org/10.1016/j.matlet.2017.09.084.
[60] K. Saware, R.M. Aurade, P. Kamala Jayanthi, V. Abbaraju, Modulatory effect of citrate reduced gold and biosynthesized silver nanoparticles on α-amylase activity, J Nanopart (2015), https://doi.org/10.1155/2015/829718.
[61] M. Wang, X. Zhou, X. Wang, M. Wang, X. Su, One-step fabrication of wavelength-tunable luminescence of gold-silver bimetallic nanoclusters: robust performance for α-glucosidase assay, Sens. Actuators B: Chem 345 (2021) 130407, https://doi.org/10.1016/j.snb.2021.130407.
[62] M. Hazarika, P.K. Boruah, M. Pal, M.R. Das, C. Tamuly, Synthesis of Pd-rGO nanocomposite for the evaluation of in vitro anticancer and antidiabetic activities, Chem. Select 4 (4) (2019) 1244–1250, https://doi.org/10.1002/slct.201802789.
[63] L.R. Lemmerman, D. Das, N. Higuita-Castro, R.G. Mirmira, D. Gallego-Perez, Nanomedicine-based strategies for diabetes: diagnostics, monitoring, and treatment, Trends Endocrinol. Metab 31 (6) (2020) 448–458, https://doi.org/10.1016/j.tem.2020.02.001.
[64] C. Ramakritinan, E. Kaarunya, S. Shankar, A. Kumaraguru, Antibacterial effects of Ag, Au and bimetallic (Ag-Au) nanoparticles synthesized from red algae, Solid State Phenom. 201 (2013) 211–230, https://doi.org/10.4028/www.scientific.net/SSP.201.211.
[65] W. Abdussalam-Mohammed, Comparison of chemical and biological properties of metal nanoparticles (Au, Ag), with metal oxide nanoparticles (ZnO-NPs) and their applications, Adv J Chem Sect A 3 (2) (2020) 111–236. https://10.33945/SAMI/AJCA.2020.2.8.
[66] M. Amina, N.M. Al Musayeib, N.A. Alarfaj, M.F. El-Tohamy, G.A. Al-Hamoud, Antibacterial and immunomodulatory potentials of biosynthesized Ag, Au, Ag-Au bimetallic alloy nanoparticles using the Asparagus racemosus root extract, Nanomaterials 10 (12) (2020) 2453, https://doi.org/10.3390/nano10122453.
[67] A. Mobed, M. Hasanzadeh, F. Seidi, Anti-bacterial activity of gold nanocomposites as a new nanomaterial weapon to combat photogenic agents: recent advances and challenges, RSC Adv. 11 (55) (2021) 34688–34698, https://doi.org/10.1039/D1RA06030A.
[68] E.A. Adebayo, J.B. Ibikunle, A.M. Oke, A. Lateef, M.A. Azeez, A.O. Oluwatoyin, A.V. AyanfeOluwa, O.T. Blessing, O.O. Comfort, O.O. Adekunle, Antimicrobial and antioxidant activity of silver, gold and silver-gold alloy nanoparticles phytosynthesized using extract of Opuntia ficus-indica, Rev. Adv. Mater. Sci. 58 (1) (2019) 313–326, https://doi.org/10.1515/rams-2019-0039.
[69] H. Jan, G. Zaman, H. Usman, R. Ansir, S. Drouet, N. Gigliolo-Guivarc'h, C. Hano, B.H. Abbasi, Biogenically proficient synthesis and characterization of silver nanoparticles (Ag-NPs) employing aqueous extract of Aquilegia pubiflora along with their in vitro antimicrobial, anti-cancer and other biological applications, J. Mater. Res. Technol. 15 (2021) 950–968, https://doi.org/10.1016/j.jmrt.2021.08.048.

[70] S. Veeramani, A.P. Narayanan, K. Yuvaraj, R. Sivaramakrishnan, A. Pugazhendhi, I. Rishivarathan, S.P. Jose, R. Ilangovan, Nigella sativa flavonoids surface coated gold NPs (Au-NPs) enhancing antioxidant and anti-diabetic activity, Process Biochem 114 (2022) 193–202, https://doi.org/10.1016/j.procbio.2021.01.004.
[71] I. Ahmad, M.N. Khan, K. Hayat, T. Ahmad, D.F. Shams, W. Khan, V. Tirth, G. Rehman, W. Muhammad, M. Elhadi, Investigating the antibacterial and anti-inflammatory potential of polyol-synthesized silver nanoparticles, ACS Omeg 9 (11) (2024) 13208–13216, https://doi.org/10.1021/acsomega.3c09851.
[72] N. Muniyappan, M. Pandeeswaran, A. Amalraj, Green synthesis of gold nanoparticles using Curcuma pseudomontana isolated curcumin: its characterization, antimicrobial, antioxidant and anti-inflammatory activities, Environ. Chem. Ecotoxicol 3 (2021) 117–124, https://doi.org/10.1016/j.enceco.2021.01.002.